Journal of Engineering Materials and Technology

Technical Brief

A Theoretical Study of the In Vivo Mechanical Properties of Angiosperm Roots: Constitutive Theories and Methods of Parameter Estimation

Alexander V. Sadovsky[1]
e-mail: sadovsky@math.uci.edu

Pierre F. Baldi
e-mail: pfbaldi@ics.uci.edu

Institute for Genomics and Bioinformatics:
Donald Bren School of Information and Computer Sciences,
University of California,
Irvine, CA 92697;
California Institute for Telecommunications and Information Technology,
University of California,
Irvine, CA 92697

Frederic Y.-M. Wan
Department of Mathematics,
School of Physical Sciences,
University of California,
267 Multipurpose Science & Technology Building,
Irvine, CA;
Department of Mechanical and Aerospace Engineering,
School of Physical Sciences,
University of California,
Irvine, CA 92697
e-mail: fwan@math.uci.edu

To investigate the constitutive relation of a plant tissue regarded as a deformable continuum, stress and strain must be determined experimentally for the same configurations. Such experiments are hindered by the inherent theoretical complexity of continuum mechanics, and by the technical difficulties of effecting external stress loads or body forces on the tissue without invasion, especially on a small scale. An understanding of appropriate mechanical problems and their solutions can help the experimentalist overcome these difficulties to a certain extent. Based on recent work on fiber-reinforced material, we formulate a constitutive theory for the root of different angiosperm species and suggest a set of loading conditions to determine the parameter values in a specific tissue sample. The loading conditions are formulated with a view toward experimental realization in vivo or with minimal invasion. For each loading condition, we formulate the corresponding mechanical problem and show how to obtain the values of the elastic parameters from known solutions. This framework can be used to analyze the interplay between mechanical and metabolic behavior in plants and to study the elastodynamics of plant tissues. [DOI: 10.1115/1.2744435]

Keywords: fiber-reinforced materials, plant mechanics, angiosperm, elongation zone, elastostatics, epidermal wall, large deformations, incompressible material, creep, boundary value problem(s) (BVP)

Introduction

The mechanical properties of a plant's tissues play a critical role in the plant's development, physiology, and survival [1–5]. Consequently, an understanding of the plant's mechanical behavior and its interplay with the genetic and physiological aspects is fundamental for basic plant science [6] and its agricultural and environmental applications. In order to test mechanical models of a biological tissue, experimental data are required. Whereas data on plant genetics and physiology abound, data on the mechanical properties of plants remain scanty. Mechanical measurements are hindered by two obstacles. First, they require a well understood mechanotheoretical framework (stress-strain relation) for the appropriate types of materials, e.g., fiber-reinforced materials [7,8]. Second, methods of exerting surface loads and body forces on a tissue fragment in vivo are difficult to find, especially on a microscopic scale. In vitro experiments aimed at measuring mechanical properties are conducted somewhat more readily [9–11], but entail substantial tissue invasion that may disturb the in vivo properties of the plant, compromising the validity of the constitutive theory the data appear to support. Despite these difficulties, in vivo experiments have been performed to measure kinematic quantities—displacements and strains—in myocardial tissue [12,13], and dynamic properties of bone surrounding a dental implant [14].

Theoretical studies of appropriate mechanical problems and their solutions can aid the experimentalist in the acquisition of the needed data. This approach has been used in various fields of biomechanical engineering (e.g., [15,16]), but has not, to our knowledge, been applied to plant mechanics.

We consider the mechanical behavior of the roots of angiosperm species. Plant biologists view such a root as a long prismatic body with circular cross section and a paraboloidal tip and divide it lengthwise into three functionally distinct regions or *zones*: the division zone, the elongation zone, and the differentiation zone (see Fig. 4 in [9]). Geometrically, the differentiation zone comprises approximately the paraboloidal tip. The immediately adjacent elongation zone is a circular cylinder of constant

[1]Corresponding author.

Contributed by the Materials Division of ASME for publication in the JOURNAL OF ENGINEERING MATERIALS AND TECHNOLOGY. Manuscript received September 21, 2006; final manuscript received March 20, 2007. Review conducted by Assimina Pelegri.

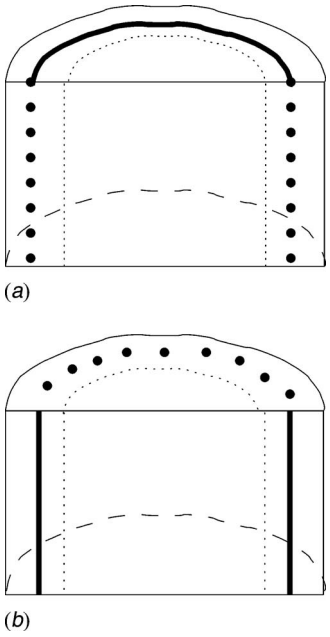

Fig. 1 Possible fiber orientations in an outer epidermal wall of a cylindrical root: (*A*) circumferential and (*B*) longitudinal

radius. In the elongation zone of the root of all angiosperm species except *Arecaceae* [9], the outer epidermal wall is lined with cellulose fibrils oriented either circumferentially (Fig. 1(*A*)) or longitudinally (Fig. 1(*B*)). It has been established experimentally that the mechanical effect of these cellulose fibrils is to act as reinforcing fibers in the medium of the tissue [17]. Mechanically, this renders the elongation zone a deformable solid cylinder with an outer, fiber-reinforced lateral layer. In this paper, we focus on determining the mechanical properties of such cylinders.

Building on the work of Horgan and Saccomandi [8], we formulate a constitutive theory for the (elongation zone of) an angiosperm root viewed as an incompressible nonlinearly elastic cylinder with an outer, fiber-reinforced layer [17] along a known direction. We then formulate three loading conditions that, on experimental implementation, would allow us to determine the parameters in the above theory. The loading conditions and the corresponding boundary value problems (BVPs) are formulated with in vivo experiments in mind. The displacements and strains are to be obtained by imaging the appropriate planar sections of the tissue in vivo, in both the undeformed and the deformed states. This can be accomplished by a number of imaging methods [18] (for methods of measuring kinematic quantities in tissues, see [12,13]). For each loading condition, we describe a method for estimating one or more of the elastic parameters involved in the constitutive model using a known (measured) solution of the corresponding BVP. The BVP presented are sufficient to determine all of the elastic parameters.

A Constitutive Theory for a Cylinder With an Outer, Fiber-Reinforced Shell Layer

In what follows, the symbols $\boldsymbol{u}$, $\mathbf{F}$, $\mathbf{B}$, $\mathbf{C}$, $\mathbf{T}$, $\mathbf{P}$, I_1 denote, respectively, the displacement field, the deformation gradient, the left Cauchy-Green strain tensor $\mathbf{B}=\mathbf{F}\mathbf{F}^T$, the right Cauchy-Green strain tensor $\mathbf{C}=\mathbf{F}^T\mathbf{F}$, the Cauchy stress tensor, the first Piola-Kirchhoff stress tensor $\mathbf{P}=(\det\mathbf{F})\mathbf{T}\mathbf{F}^{-T}$, and the invariant $\mathrm{tr}\,\mathbf{C}$ of $\mathbf{C}$. The reference (deformed) configuration of a cylinder will be described using the polar cylindrical coordinates (R,Θ,Z) $((r,\theta,z))$ with the corresponding mobile basis $\hat{R},\hat{\Theta},\hat{Z}$ $(\hat{r},\hat{\theta},\hat{z})$. The operator $\boldsymbol{\nabla}$ denotes the gradient in the material coordinates. Given a material point $\boldsymbol{X}$ with coordinates (R,Θ,Z) in the reference configuration,

$$\boldsymbol{\chi}(\boldsymbol{X})=\boldsymbol{\chi}(T,\Theta,Z):=\boldsymbol{X}+\boldsymbol{u}(\boldsymbol{X}) \tag{1}$$

where, $\boldsymbol{\chi}$ denotes the deformation mapping.

A constitutive theory proposed by Horgan and Saccomandi [8] for an incompressible nonlinearly elastic material reinforced by a family of fibers along a direction specified by a unit vector $\hat{a}_0$ in the reference configuration is given by the strain-energy density function

$$W=\frac{\mu}{2}(I_1-3)-\nu J_m\left\{(I_4-1)+J_m\ln\left(1-\frac{I_4-1}{J_m}\right)\right\}, \tag{2}$$

where $I_4=\hat{a}_0\cdot\mathbf{C}\hat{a}_0$, μ is the shear modulus for infinitesimal strains in the absence of anisotropies, ν is a shear modulus that serves as a measure of anisotropy, and J_m is a dimensionless parameter that reflects the degree of rigidity of the fiber reinforcement. Set $\boldsymbol{a}=\mathbf{F}\hat{a}_0$. The Cauchy stress corresponding to (2) is given (see Eq. (28) in [8]) by

$$\mathbf{T}=-p\mathbf{I}+\mu\mathbf{B}+2\nu\frac{J_m(I_4-1)}{J_m-(I_4-1)}\boldsymbol{a}\otimes\boldsymbol{a} \tag{3}$$

where p is a hydrostatic pressure to be determined.

Consider a circular cylinder with cross section of constant radius $R=a$ and with an outer epidermal wall $(1-\alpha)<R/a<1$ (α a constant $<1/2$) reinforced by a single family of fibers directed along either $\hat{\Theta}$ (Fig. 1(*A*)) or $\hat{Z}$ (Fig. 1(*B*)).

The rest of the body is homogeneous and isotropic. The specific directions of the fibers are assumed known from experiments [19]. A constitutive theory for such a cylinder is given by the generalization

$$\mathbf{T}=-p\mathbf{I}+\mu\mathbf{B}+2\nu(R)\frac{J_m(I_4-1)}{J_m-(I_4-1)}\boldsymbol{a}\otimes\boldsymbol{a} \tag{4}$$

of (3), with the anisotropy parameter ν now being a suitable function of R taking values in an interval $[0,\nu^0]$ and satisfying the condition that there exist a small positive $\epsilon\ll\alpha$ such that

$$\nu(R)=0 \text{ for } R/a<(1-\alpha-\epsilon), \text{ and}$$

$$\nu(R)=\nu^0>0 \text{ for } R/a>(1-\alpha+\epsilon) \tag{5}$$

The parameter α characterizes the thickness of the fiber-reinforced outer cell layer and will be assumed known, as it can be independently determined by experiments [20]. The value $1/\epsilon$ characterizes the accuracy with which $\nu(R)/\nu^0$ approximates the characteristic function of the fiber-reinforced part of each cross section $Z=$const.: as $\epsilon\to0$, the smooth function $\nu(R)$ uniformly approaches the step function that equals 0 on $0<R/a<1-\alpha$ and equals ν^0 on $1-\alpha\le R/a<1$.

For small deformations, the linearized Lagrange-Green strain tensor $\mathbf{E}=\frac{1}{2}(\boldsymbol{\nabla}\otimes\boldsymbol{u}+\boldsymbol{\nabla}\otimes\boldsymbol{u}^T)$ is used to approximate each of $\mathbf{B},\mathbf{C}$ by $\mathbf{I}+2\mathbf{E}$. This yields the linearization

$$\mathbf{T}=-p\mathbf{I}+\mu(\mathbf{I}+2\mathbf{E})+4\nu(R)[\hat{a}_0\cdot(\mathbf{E}\hat{a}_0)]\hat{a}_0\otimes\hat{a}_0 \tag{6}$$

of (4). Notice that the parameter J_m no longer appears. Furthermore, since the hydrostatic pressure p is undetermined (being the Lagrange multiplier corresponding to the constraint of incompressibility), the term $\mu\mathbf{I}$ can be absorbed into the hydrostatic pressure term $-p\mathbf{I}$, yielding the linearized Cauchy stress tensor

$$\mathbf{T}=-p\mathbf{I}+2\mu\mathbf{E}+4\nu(R)[\hat{a}_0\cdot(\mathbf{E}\hat{a}_0)]\hat{a}_0\otimes\hat{a}_0 \tag{7}$$

We now formulate loading conditions and the corresponding BVPs for measuring the elastic parameters μ, ν^0, and J_m for a fixed choice of the function $\nu(R)$ satisfying condition (5). Each formulation is followed by a description of a mathematical procedure for determining the relevant parameters. In these procedures,

the hydrostatic pressure, p, is assumed known (i.e., experimentally measurable in advance), which facilitates the computation of the elastic parameters. The situation where p is not known in advance is addressed in a later section.

Loading Conditions, the Corresponding BVP, and Methods of Fitting the Parameters

In the coordinates (R,Θ,Z), the elongation zone of the angiosperm root, which serves as the physical domain of the BVP below, is a circular cylinder $\Omega_L: R<a, |Z|<L$ of finite length $2L$. Although the cylinder is long and may well admit the idealization of an infinite cylinder, we do not resort to this idealization here, for lack of mechanical data. Instead, we assume known displacement fields $\boldsymbol{U}^+$, $\boldsymbol{U}^-$ on the respective bases $z=L$, $z=-L$. Since the displacements $\boldsymbol{U}^+$, $\boldsymbol{U}^-$ are purely kinematic quantities, their experimental determination requires no knowledge of the root's mechanical properties and no actual removal of the elongation zone from the root.

Throughout this section, assume Ω_L obeys the constitutive theory (4) or, for small deformations, the linearized constitutive theory (7). The direction $\hat{a}_0$ will be specified for each loading condition. The symbol $\delta'\Omega_L$ denotes the lateral surface of Ω_L in the *deformed* configuration, i.e., the image of the material surface $R=a$ under the deformation (1).

Loading Condition 1. Circumferentially or Longitudinally Oriented Fibers: A Band of Load, Small Deformations. Let $\hat{a}_0$ be either $\hat{\Theta}$ or $\hat{Z}$. A band of width $2h$, $h \ll L$, is shrunk around the cylinder as shown in Fig. 2(*A*), effecting an external normal stress load at $(R=a, |Z|<h)$ of constant magnitude S_o. By axial symmetry and invariance under the reflections through the planes $\Theta=$const, the displacement field has the form $\boldsymbol{u}(R,Z)=u_R(R,Z)\hat{R}+u_Z(R,Z)\hat{Z}$. Since the deformations are small, we assume the linearized constitutive theory (7). The material coordinates are thus identified with the spatial ones; the Cauchy stress, with the first Piola-Kirchhoff stress.

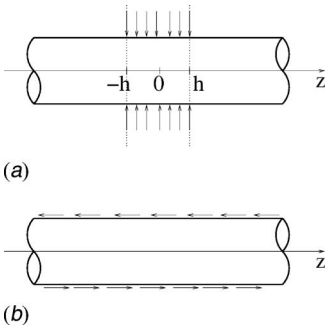

Fig. 2 A portion of the cylinder Ω_L near the cross section $z=0$ under different loading conditions. (*A*) Loading condition 1. Constriction of the cylinder Ω_L by a shrinking band, shown in longitudinal section: The normal stress load $\mathbf{T}\cdot\hat{r}|_{r=a}$ equals $-S_0\hat{r}$ at $r=a, |z|<h$, and equals zero on the remaining portion of the lateral surface. (*B*) Loading condition 2. The lateral surface of the cylinder is subjected to the external stress loads $\pm S_0\hat{z}$ applied, respectively, at the lines $r=a, \theta=\pm\pi/2$.

A two-dimensional projection of a three-dimensional incompressible material is generally not incompressible. However, the deformation corresponding to the above special form of $\boldsymbol{u}$ maps a material element of volume $R\,dR\,d\Theta\,dZ$ to one of the same volume $r\,dr\,d\theta\,dz$, where, by radial symmetry, $d\theta=d\Theta$. Therefore, $r\,dr\,dz=R\,dR\,dZ$, i.e., *the resulting deformation of the representative* (R,Z) *plane is incompressible*.

We obtain a BVP which consists in finding the displacement $\boldsymbol{u}(R,Z)=u_r(R,Z)\hat{r}+u_z(R,Z)\hat{z}$ and the hydrostatic pressure $p(R,Z)$ satisfying

$$\nabla\cdot\mathbf{P}=\mathbf{0} \quad \text{(equilibrium)} \quad \det\mathbf{B}=1 \quad \text{(incompressibility)} \tag{8}$$

$$\begin{aligned}
&u_r|_{r=0}=0 \qquad \delta_r p|_{R=0}=0 && \text{(axial symmetry)}\\
&\delta_z u_z|_{Z=0}=0 \qquad \delta_z p|_{Z=0}=0 && \text{(invariance under } Z\mapsto -Z)\\
&\mathbf{T}\cdot\hat{r}|_{\delta'\Omega_L}=\begin{cases}-S_0\hat{R} & \text{for } |Z|\le h\\ \mathbf{0} & \text{for } |Z|>h\end{cases} && \text{(loading by the shrinking band)}\\
&\boldsymbol{u}|_{z=\pm L}=\boldsymbol{U}^{\pm} && \text{(displacements on bases known)}
\end{aligned} \tag{9}$$

A solution of the above BVP gives the displacement $\boldsymbol{u}(R,Z)$ and $p(R,Z)$, hence, also the components of the strain tensor $\mathbf{E}(R,Z)$. By (7), the boundary condition on T_{rr} at the points $Z=0$ of the surface $\delta'\Omega_L$ implies

$$T_{rr}(a,0)=P_{rr}(a,0)=-p(a,0)+2\mu E_{rr}(a,0)=-S_0$$

whence

$$\mu=\frac{p(a,0)-S_0}{2E_{rr}(a,0)} \tag{10}$$

Similarly, the hoop stress and strain at $(R,Z)=(a,0)$ satisfy

$$\begin{aligned}
0=T_{\theta\theta}(a,0)&=-p(a,0)+[2\mu+4\nu(a)]E_{\theta\theta}(a,0)\\
&=-p(a,0)+[2\mu+4\nu^0]E_{\theta\theta}(a,0) \quad \text{(by condition(5))}
\end{aligned}$$

With μ known from (10) and with $E_{\theta\theta}(a,0)\neq 0$ (since $u_r(a,0)<0$), the parameter ν^0 is determined by

$$\nu^0=\frac{\mu}{2}+\frac{p(a,0)}{4E_{\theta\theta}(a,0)} \tag{11}$$

Loading Condition 2. Circumferentially Oriented Fibers: Longitudinal Shear Stress, Large Deformations. Assume here $\hat{a}_0=\hat{\Theta}$. Along the line $R=a$, $\Theta=\pi/2$ (resp., $R=a$, $\Theta=-\pi/2$), apply the stress load $S_0\hat{Z}$ (resp., $-S_0\hat{Z}$), with S_0 assumed positive for definiteness.

Since the deformations are large, the adequate constitutive relation is (4) with $\hat{a}_0=\hat{\Theta}$,

$$\mathbf{T}=-p\mathbf{I}+\mu\mathbf{B}+2\nu(R)\frac{J_m(I_4-1)}{J_m-(I_4-1)}(\mathbf{F}\hat{\Theta})\otimes(\mathbf{F}\hat{\Theta})$$

By symmetry, the corresponding mechanical BVP is set in the domain $0<\Theta<\pi/2$ of the reference configuration and consists in solving Eqs. (8) subject to the boundary conditions

$$\boldsymbol{u}|_{Z=\pm L}=\boldsymbol{U}^{\pm} \quad \delta_{\Theta}u_R|_{\Theta=0,\pi/2}=0 \quad u_{\Theta}|_{\Theta=0,\pi/2}=0$$

$$\mathbf{T}\cdot\hat{r}|_{\delta'\Omega_L}=\delta\left(\theta-\frac{\pi}{2}\right)S_0\hat{z} \tag{12}$$

From the boundary conditions and from the symmetry condition $\delta_Z\boldsymbol{u}=\mathbf{0}$ at the material point $\boldsymbol{X}_0$ with coordinates $(R,\Theta,Z)=(a,\pi/2,0)$ and with the image $\boldsymbol{x}_0=\boldsymbol{\chi}(\boldsymbol{X}_0)$ under the deformation (1), it follows that $\hat{r}(\boldsymbol{x}_0)=\hat{R}(\boldsymbol{X}_0)$ and $\hat{z}(\boldsymbol{x}_0)=\boldsymbol{Z}(\boldsymbol{X}_0)$. Noting this and substituting the solution $\boldsymbol{u}$ of the above problem into the last of the boundary conditions (12), we obtain, at $\boldsymbol{x}_0'$, the equation

$$S_0=T_{zr}=\mu B_{zr}+2\nu^0\frac{J_m(I_4-1)}{J_m-(I_4-1)}\{\hat{z}\cdot[(\mathbf{F}\hat{\theta}\otimes\mathbf{F}\hat{\theta})\cdot\hat{r}]\} \tag{13}$$

The value of J_m is the only unknown in (13) and can therefore be found by direct computation.

Loading Condition 3. Longitudinally Oriented Fibers, Simple Torsion, Large Deformations. Taking $\hat{a}_0=\hat{Z}$ in (4), we obtain the constitutive theory

$$\mathbf{T}=-p\mathbf{I}+\mu\mathbf{B}+2\nu(R)\frac{J_m(I_4-1)}{J_m-(I_4-1)}(\mathbf{F}\hat{z})\otimes(\mathbf{F}\hat{z}) \tag{14}$$

The parameters μ,ν^0 are assumed known, since, given a successful experimental setup, they can be determined from experiments corresponding to loading condition 1 with $\hat{a}_0=\hat{Z}$.

In order to find J_m, we propose to subject Ω_L to a twisting couple so that (a) Ω_L is in equilibrium, (b) the lateral surface of Ω_L is traction free, (c) the bases $Z=\pm L$ experience the resultant torques $\boldsymbol{M}$, and (d) the section $Z=0$ undergoes zero displacement. The resulting displacement field in Ω_L has the purely circumferential form $\boldsymbol{u}(R,Z)=R\tau(R)Z\hat{\Theta}$, and the corresponding BVP consists of the Eqs. (8) subject to the boundary conditions

$$\mathbf{T}\cdot\hat{n}|_{\delta'\Omega_L}=\mathbf{T}\cdot\hat{r}|_{\delta'\Omega_L}=\mathbf{0} \quad \mathbf{T}\cdot\hat{n}|_{z=\pm L}=\pm t^0(r)\hat{\theta} \tag{15}$$

The function $t^0(r)$, unknown in detail, gives at each cross section $A:z=z_0$ the known resultant torque

$$\boldsymbol{M}=\int_A(\boldsymbol{x}-z_0\hat{z})\times[\mathbf{T}(\boldsymbol{x})\cdot\hat{z}]dA(\boldsymbol{x}) \quad dA=r\,dr\,d\theta \tag{16}$$

where the point represented by the vector $\boldsymbol{x}$ varies over A. The stress vector $\mathbf{T}(\boldsymbol{x})\cdot\hat{z}$ at $z=0$ has components

$$T_{zr}=0 \quad T_{z\theta}=\frac{r\mu\tau(r)+2J_mr^3\nu(R)\tau(r)^3}{J_m-r^2\tau(r)^2}$$

$$T_{zz}=\frac{\mu-p(r)+2J_mr^2\nu(R)\tau(r)^2}{J_m-r^2\tau(r)^2}$$

Substituting these quantities and the components $x_r=r\cos\theta, x_\theta=r\sin\theta, x_z=0$ of $\boldsymbol{x}$ into the left-hand side of (16) with $z_0=0$ and taking the scalar product with $\hat{z}$, we obtain the equation

$$\hat{z}\cdot\boldsymbol{M}=\int_{z_0=0}(x_rT_{z\theta}-x_\theta T_{zr})dA(\boldsymbol{x}) \tag{17}$$

which can be used to find J_m iteratively.

A Method for Finding the Elastic Parameters When the Hydrostatic Pressure is Unknown

The demonstrated methods of determining the elastic parameters are based on the assumption that the hydrostatic pressure p in (4) is known—i.e., can be determined experimentally—in advance. This allows the parameters μ, ν^0, and J_m to be determined from Eqs. (10), (11), (13), and (17). In cases where prior knowledge of p is not available, the elastic parameters can be sought iteratively. To carry this out, one must solve an inverse problem. While such problems are generally difficult, the particular loading conditions presented above allow for the following systematic approach.

Consider loading condition 1 above. We note that (a) a measured value $\mathbf{E}^{\text{meas}}(\boldsymbol{s})$ of the strain tensor $\mathbf{E}(\boldsymbol{s})$ at each spatial point $\boldsymbol{s}$ can be obtained—without knowing the values of the elastic parameters—by imaging the deformation in the tissue caused by the loading condition, and that (b) each choice of the values (μ,ν^0) yields, through the solution of the BVP (8) and (9), the computed values $E_{rr}^{\text{comp}},E_{\theta\theta}^{\text{comp}}$ of the corresponding strain components. We may therefore write

$$E_{rr}^{\text{comp}}=E_{rr}^{\text{comp}}(\mu,\nu^0;\boldsymbol{s}) \quad E_{\theta\theta}^{\text{comp}}=E_{\theta\theta}^{\text{comp}}(\mu,\nu^0;\boldsymbol{s})$$

and, fixing a spatial point $\boldsymbol{s}_0$, introduce the vector-valued function

$$\vec{\phi}(\mu,\nu^0)=[E_{rr}^{\text{comp}}(\mu,\nu^0;\boldsymbol{s}_0)-E_{rr}^{\text{meas}}(\boldsymbol{s}_0),E_{\theta\theta}^{\text{comp}}(\mu,\nu^0;\boldsymbol{s}_0)-E_{\theta\theta}^{\text{meas}}(\boldsymbol{s}_0)] \tag{18}$$

computable at least numerically, and sufficiently smooth in μ,ν^0 provided the BVP is well posed. (Instead of evaluating the computed strains at a fixed spatial point, it may be desirable to average them over a fixed sample $\boldsymbol{s}^j(j=1,\ldots,N)$ of spatial points. Thus, for example, instead of $E_{rr}^{\text{comp}}(\mu,\nu^0;\boldsymbol{s}_0)$, the value $(1/N)\Sigma_jE_{rr}^{\text{comp}}(\mu,\nu^0;\boldsymbol{s}^j)$ would be used.)

Our task, then, is to find a zero (μ_*,ν_*^0) of $\boldsymbol{\phi}(\mu,\nu^0)$. Pursuing this task by Newton's Method, we see that a kth guess (μ_k,ν_k^0) at (μ_*,ν_*^0) can be corrected to obtain a better guess (μ_{k+1},ν_{k+1}^0) by the means of the formula

$$(\mu_{k+1},\nu_{k+1}^0)=(\mu_k,\nu_k^0)-[\boldsymbol{\phi}'(\mu_k,\nu_k^0)]^{-1}\boldsymbol{\phi}(\mu_k,\nu_k^0)$$

where the total derivative $\boldsymbol{\phi}'(\mu_k,\nu_k^0)$ can be approximated numerically using finite differences. This procedure, assuming Newton's Method converges, yields an approximation of (μ_*,ν_*^0).

Each of the remaining loading conditions can be handled similarly, by seeking a zero of the function

$$\boldsymbol{\phi}(\mu,\nu^0,J_m)=[E_{rr}^{\text{comp}}(\mu,\nu^0,J_m;\boldsymbol{s}_0)-E_{rr}^{\text{meas}}(\boldsymbol{s}_0),E_{\theta\theta}^{\text{comp}}(\mu,\nu^0,J_m;\boldsymbol{s}_0)-E_{\theta\theta}^{\text{meas}}(\boldsymbol{s}_0),E_{zz}^{\text{comp}}(\mu,\nu^0,J_m;\boldsymbol{s}_0)-E_{zz}^{\text{meas}}(\boldsymbol{s}_0)]$$

The disadvantage of the above method is the potentially high computational cost: the kth iteration requires that ϕ be evaluated some finite number M of times, with M independent of k. Each evaluation, in turn, requires the solution of the corresponding BVP.

Conclusion

We have formulated a constitutive theory for the elongation zone of the angiosperm root and loading conditions that, on successful experimental implementation, would yield estimates of the mechanical parameters. This framework may guide the experimentalist's efforts and serve as a beginning for further quantitative studies of the interplay in plant tissues between mechanics and various biological processes, see, e.g., [21,22].

An individual trial of each experiment suggested by the above loading conditions produces data only on the elastostatic properties of the tissue fragment being examined. To obtain information on the viscous and plastic properties [23] of the tissue, one must carry out an appropriately timed sequence of trials for the given static experiment (e.g., [9]), each trial accompanied by imaging the relevant sections of the deformed tissue. Such a sequence of trials may consist either of briefly subjecting the tissue to a static load, or of maintaining the prescribed surface loads or body forces for the entire duration of the experiment. The latter approach can yield information on creep [23]. The technology used in [14] can be used to exert external concentrated stress loads in vivo on the tissue types discussed in this paper.

A phenomenon of high interest to the plant biology community, especially at the cellular level, is the interplay between the mechanical behavior and biological processes (see, for example, [22,24,25]. To investigate this phenomenon, one may embed a constitutive theory such as the one presented here in a model where the mechanical parameters evolve with time depending on the concentrations of various molecule types in the tissue.

Acknowledgment

We were supported by the National Institutes of Health, National Research Service Award 5 T15 LM007443 from the National Library of Medicine, awarded to P. Baldi. The research of F.Y.M. Wan was supported by UC Irvine Research Grant 445861. The authors thank G. Kassab for useful suggestions on the choice and structure of content for the manuscript.

References

[1] Bengough, A. G., Bransby, M. F., Hans, J., McKenna, S. J., Roberts, T. J., and Valentine, T. A., 2006, "Root Responses to Soil Physical Conditions; Growth Dynamics From Field to Cell," J. Exp. Bot., **57**(2), pp. 437–447.

[2] Hanbury, C. D., and Atwell, B. J., 2005, "Growth Dynamics of Mechnially Impeded Lupin Roots: Does Altered Morphology Induce Hypoxia?," Ann. Bot. (London), **96**(5), pp. 913–924.

[3] Hamman, K. D., Williamson, R. L., Steffer, E. D., Wright, C. T., Hess, J. R., and Profogle, P. A., 2005, "Structural Analysis of Wheat Steams," Appl. Biochem. Biotechnol., **121-124**, pp. 71–80.

[4] Spatz, H.-C., and Emanns, A., 2004, "The Mechnical Role of the Endodermis in Equisetum Plant Stems," Am. J. Bot., **91**, pp. 1936–1938.

[5] Spatz, H.-C., and Brüchert, F., 2000, "Basic Biomechanics of Self-Supporting Plants: Wind Loads and Gravitational Loads on a Norway Spruce Tree," Forest Ecol. Manage., **135**, pp. 33–44.

[6] Niklas, K. J., 1992, *Plant Biomechanics: An Engineering Approach to Plant Form and Function*, The University of Chicago Press.

[7] Spencer, A. J. M., 1984, *Continuum Theory of the Mechanics of Fibre-Reinforced Composites*, New York: Springer-Verlag.

[8] Horgan, C. O., and Saccomandi, G., 2005, "A New Constitutive Theory for Fiber-Reinforced Incompressible Nonlinearly Elastic Solids," J. Mech. Phys. Solids, **53**, pp. 1985–2015.

[9] Kerstens, S., and Verbelen, J. P., 2002, "Cellulose Orientation in the Outer Epidermal Wall of Angiosperm Roots: Implications for Biosystematics," Ann. Bot. (London), **90**, pp. 669–676.

[10] Berge, H., Spatz, H. C., Speck, T., and Neinhuis, C., 2004, "Two-dimensional Tension Tests in Plant Biomechanics–Sweet Cherry Fruit Skin as a Model System," Plant Biol. (Stuttg), **6**(4), pp. 432–439.

[11] Blahovec, J., 1996, "Stress Relaxation in Cherry Fruit," Biorheology, **33**(6), pp. 451–462.

[12] Amundsen, B. H., Helle-Valle, T., Edvardsen, T., Torp, H., Crosby, J., Lyseggen, E., Stoylen, A., Ihlen, H., Lima, J. A., Smiseth, O. A., and Slordahl, S. A., 2006, "Noninvasive Myocardial Strain Measurement by Speckle Tracking Echocardiography: Validation Against Sonomicrometry and Tagged Magnetic Resonance Imaging," J. Am. Coll. Cardiol. **47**(4), pp. 789–793.

[13] Rodriguez, I., Ennis, D. B., and Wen, H., 2006, "Noninvasive Measurement of Myocardial Tissue Volume Change During Systolic Contraction and Diastolic Relaxation in the Canine Left Ventricle," Magn. Reson. Med., **55**(3), pp. 484–490.

[14] Barzin, A., Sheets, C. G., and Earthman, J. C., 2002, "Mechanical Biocompatibility of Dental Implant Materials," *Proceedings of the Fourth Pacific Rim, International Conference on Materials*, Japanese Institute of Metals, pp. 2492–2952.

[15] Fung, Y. C., and Liu, S. Q., 1995, "Determination of the Mechanical Properties of the Different Layers of Blood Vessels *In Vivo*," Proc. Natl. Acad. Sci. U.S.A., **92**(6), pp. 2169–2173.

[16] Baek, S., Rajagopal, K. R., and Humphrey, J. D., 2006, "A Theoretical Model of Enlarging Intracranial Fusiform Aneurysms," J. Biomech. Eng., **128**(1), pp. 142–149.

[17] Kerstens, S., Decraemer, W. F., and Verbelen, J. P., 2001, "Cell Walls at the Plant Surface Behave Mechanically Like Fiber-Reinforced Composite Materials," Plant Physiol., **127**, pp. 381–385.

[18] Sharpe, J., 2004, "Optical Projection Tomography," Annu. Rev. Biomed. Eng., **6**, pp. 209–228.

[19] Verbelen, J. P., and Kerstens, S., 2000, "Polarization Confocal Microscopy and Congo Red Fluorescence: A Simple and Rapid Method to Determine the Mean Cellulose Fibril Orientation in Plants," J. Microsc., **198**(2), pp. 101–107.

[20] Sugimoto, K., Williamson, R. E., and Wasteneys, G. O., 2000, "New Techniques Enable Comparative Analysis of Microtubule Orientation, Wall Texture, and Growth Rate in Intact Roots of *Arabidopsis*," Plant Physiol., **124**(4), pp. 1493–1506.

[21] Shimazaki, Y., Ookawa, T., and Hirasawa, T., 2005, "The Root Tip and Accelerating Region Suppress Elongation of the Decelerating Region without any Effects on Cell Turgor in Primary Roots of Maize under Water Stress," Plant Physiol., **139**, pp. 458–465.

[22] Verbelen, J. P., Vissenberg, K., Kerstens, S., and Le, J., 2001, "Cell Expansion in the Epidermis: Microtubules, Cellulose, Orientation and Wall loosening Enzymes," Journal of Plant Physiology, **158**(5), pp. 537–543.

[23] Spencer, A. J. M., 2004, *Continuum Mechanics*, Dover.

[24] Kaku, T., Tabuchi, A., Wakabayashi, K., Kamisaka, S., and Hoson, T., 2002, "Action of Xyloglucan Hydrolase within the Native Cell Wall Architecture and Its Effect on Cell Wall Extensibility in Azuki Bean Epicotyls," Plant Cell Physiol., **43**(1), pp. 21–26.

[25] Yuan, S., Wu, Y., and Cosgrove, D. J., 2001, "A Fungal Endoglucanase with Plant Cell Wall Extension Activity," Plant Physiol., **127**(1), pp. 324–333.